

# Consecutive Conformational Transitions and Deaggregation of Multiple-Helical Poly(diacetylene)s

Jan Weiss,<sup>†</sup> Eike Jahnke,<sup>†</sup> Nikolai Severin,<sup>‡</sup> Jürgen P. Rabe,<sup>‡</sup> and Holger Frauenrath<sup>\*†</sup>

ETH Zürich, Department of Materials, Wolfgang-Pauli-Str. 10, HCI H515, 8093 Zürich, Switzerland; and Humboldt University Berlin, Department of Physics, Newtonstr. 15, 12489 Berlin, Germany

Received February 18, 2008

## ABSTRACT

The polymerization of diacetylene macromonomers based on oligopeptide–polymer conjugates yields conjugated polymers with multiple-helical quaternary structures. These polymers exhibit a rich dynamic folding behavior upon the addition of protic cosolvents. Thus, a helix–helix transition under helix-sense inversion was followed by a reversible helix–coil transition. Both transitions involved changes in the aggregation state of the multiple-helical superstructures. The resemblance of the observed consecutive and cooperative conformational transitions to those of biopolymers underlines the importance of supramolecular self-assembly as a pathway toward biofunctional materials with optoelectronic activity.

An important factor responsible for the nanostructure formation observed in biomaterials and for their often remarkable properties is the ability of the constituting biopolymers to undergo dynamic folding in solution and attain well-defined hierarchical structures.<sup>1</sup> Successful attempts to replicate this kind of higher order structure formation in synthetic polymers are still limited in scope.<sup>2,3</sup> One promising strategy is the foldamer approach<sup>4–7</sup> also applied in the preparation of folded poly(acetylene)s,<sup>8–13</sup> as a prominent class of  $\pi$ -conjugated foldamers. Nevertheless, the highly desirable preparation of hierarchically structured, optoelectronically active polymers makes the exploration of complementary synthetic strategies an attractive research goal. In this context, we recently demonstrated how supramolecular self-assembly can be utilized as the first step in the preparation of hierarchically structured  $\pi$ -conjugated polymers.<sup>14</sup> Thus, diacetylene macromonomers with oligopeptide–polymer conjugate substituents such as **1**–**3** were designed to self-assemble into high aspect ratio supramolecular polymers (Chart 1).<sup>15</sup> In contrast to previous investigations of diacetylene polymerizations in either vesicular aggregates<sup>16–22</sup> or hydrogen-bonded organogels,<sup>23–28</sup> these supramolecular polymers were obtained via parallel  $\beta$ -sheet formation as a precise secondary structure formation mechanism. They exhibited a uniform diameter on the order of the molecular length scale and were consti-

tuted from a known, finite number of (two or four) laminated  $\beta$ -sheet *tapes* controlled by the pattern of the N–H···O=C hydrogen bonding sites.<sup>29,30</sup> The supramolecular polymers were then converted into  $\pi$ -conjugated polymers under retention of their previously assembled higher order structures, yielding well-defined quadruple-helical (**P1**) or double-helical poly(diacetylene)s (**P3**) in solution.<sup>31</sup>

In the present paper, we report on multiple-helical superstructures and conformational transitions of the poly(diacetylene)s **P1** and **P2** in solution, the latter of which contained the Fmoc group as an additional UV chromophore. Upon addition of hydrogen-bond breaking cosolvents, the multiple-helical polymers underwent two consecutive and cooperative solvatochromic transitions. UV, CD, and Raman spectroscopy in combination with scanning force microscopy (SFM) imaging allowed us to identify these as a helix–helix transition followed by a reversible helix–coil conversion, the former of which proceeded under helix-sense inversion in the case of **P1**. Furthermore, both transitions involved a controlled (reversible) deaggregation of the multiple-helical superstructures. Hence, the hierarchically structured poly(diacetylene)s **P1** and **P2** exhibited a dynamic folding behavior similar to biopolymers. Moreover, they helped to gain insight into the nature of the poly(diacetylene) solvatochromism.<sup>32–37</sup>

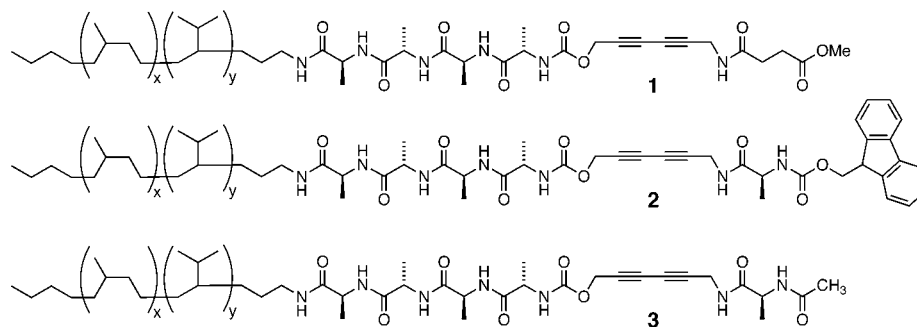
Macromonomers **1** and **2** were synthesized as described previously.<sup>31</sup> **1** had been observed to self-organize in organic solvents into right-handed double-helical fibrils constituted

\* Corresponding author. E-mail: frauenrath@mat.ethz.ch. Telephone: (+41) 44 633 6474. Fax: (+41) 44 633 1390.

<sup>†</sup> ETH Zürich, Department of Materials.

<sup>‡</sup> Humboldt University Berlin, Department of Physics.

Chart 1



from two *ribbon* substructures, which, in turn, were formed from two single parallel  $\beta$ -sheet *tapes*.<sup>14</sup> Similarly, the Fmoc-terminated macromonomer **2** was found to attain the expected predominantly parallel  $\beta$ -sheet secondary structures, as confirmed by IR spectroscopy.<sup>38</sup> SFM images of **2** on a monolayer of flat lying stearyl amines on highly oriented pyrolytic graphite (HOPG)<sup>39</sup> revealed the presence of filamental features extending over several micrometers, the majority of which were left-handed helically twisted *ribbons*<sup>40,41</sup> (Figure 1a,b) with a complex periodic fine structure very similar to its acetylated sibling **3**, as expected from their identical pattern of N–H $\cdots$ O=C hydrogen bonding sites.<sup>29</sup> Interestingly, some *ribbons* were unwound at their ends (Figure 1c,d), which, for the first time, unambiguously demonstrated that they were indeed constituted from two flat substructures with dimensions as expected for single  $\beta$ -sheet *tapes*.<sup>38</sup> Finally, a minor population of, likewise, left-handed helical *ribbons* with a similar width and height, but a more tightly wound helical fine structure, was also observed (Figure 1e).

For the topochemical diacetylene polymerization<sup>42</sup> within the self-assembled aggregates, the clear and colorless dilute solutions of **1** or **2** in chloroform or dichloroethane (DCE), which did not show any tendency to form gels under the applied conditions, were subjected to UV irradiation and instantaneously attained an intense blue-purple color, which further intensified over time. The UV spectra (Figures 2b, 3b) were consistent with the formation of the corresponding poly(diacetylene)s **P1** and **P2**, and the Raman spectra (Figures 2c, 3c) allowed us to straightforwardly assign the observed UV band structure of **P1** as vibronic side bands of only one poly(diacetylene) species. By contrast, the freshly polymerized **P2** appeared to be already a mixture with the red form of **P2** (vide infra). CD spectroscopy (Figures 2a, 3a) did not only prove that the polymerization inside the multiple-helical supramolecular polymers produced  $\pi$ -conjugated polymers with homochiral superstructures in both cases but, more importantly, that **P1** and **P2** attained superstructures with an opposite helix sense in solution. Thus, both **P1** and **P2** exhibited bisignate CD signals with zero-crossings at the positions of the respective highest wavelength UV absorptions but with a *positive* Cotton effect for **P1** and a *negative* one for **P2**. Likewise, the CD activities near the respective lower wavelength UV absorption maxima were *negative* for **P1**, and *positive* for **P2**. Hence, the opposite helix sense of the supramolecular polymers from **1** and **2**

observed in the SFM images found a perfect reflection in the clean CD signatures of the corresponding poly(diacetylene)s **P1** and **P2**, which represents one of the first examples of a direct correlation between the CD activity of a conjugated polymer backbone with its *known* superstructure as evidenced by SFM imaging.<sup>36,37,43–48</sup> As the SFM images before and after UV irradiation were virtually identical, the polymerization can, furthermore, be assumed to proceed

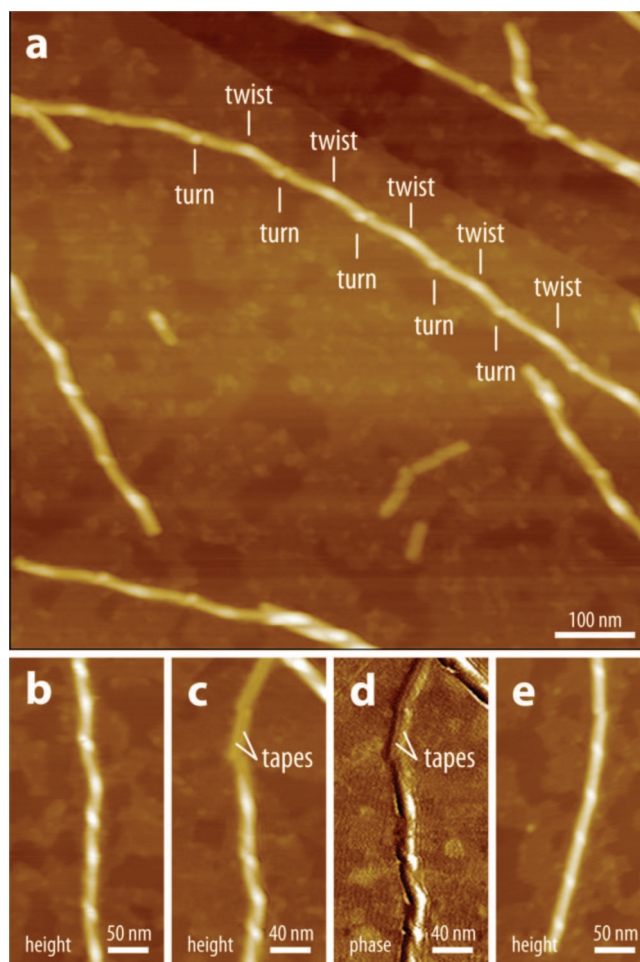


**Figure 1.** SFM images of **2** on a monolayer of flat lying stearyl amine on HOPG showed left-handed helical *ribbons* the majority of which (a,b) exhibited a periodic fine structure with an identity period of  $114 \pm 19$  nm, where features reminiscent of “helix turns” alternated with broader “twists”; (c,d) these *ribbons* were constituted from two single  $\beta$ -sheet *tape* substructures; (e) a minor population of *ribbons* exhibited left-handed “helix turn” features placed at a distance of  $64 \pm 6$  nm.<sup>38</sup>

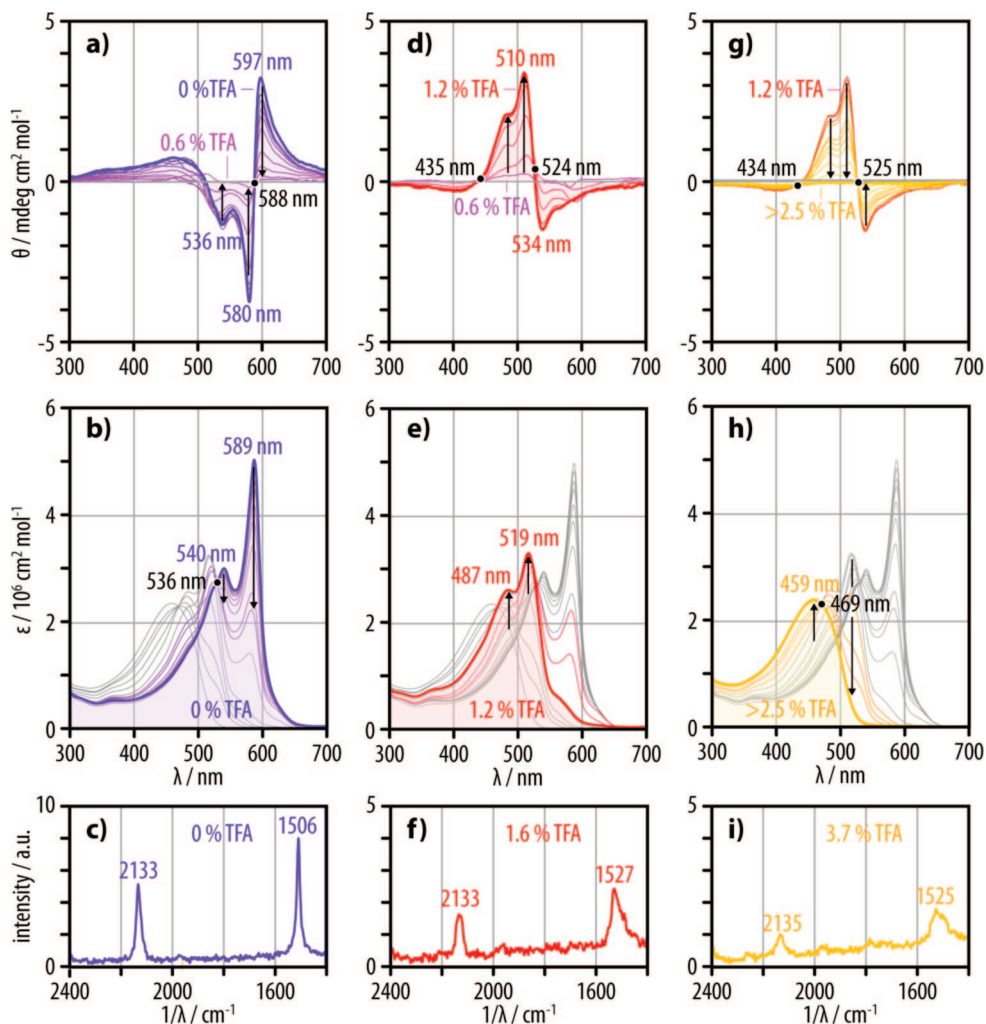


**Figure 2.** CD, UV, and Raman spectra of (a–c) the blue-purple solutions of **P1** after polymerization were consistent with the presence of only one species in DCE solution, exhibiting a *positive* Cotton effect; the addition of up to 0.6 vol % TFA led to a preliminary loss in CD activity before (d–f) a solvatochromic transition to the red form occurred at around 1.2 vol % TFA, which showed a *negative* Cotton effect; (g–i) addition of more TFA yielded the CD inactive yellow form.<sup>38</sup>

under retention of the superstructures already existing in solution.

Upon the addition of trifluoroacetic acid (TFA) as a hydrogen bond breaking cosolvent, both **P1** (Figure 2) and **P2** (Figure 3) were found to undergo two successive solvatochromic transitions. Remarkably, the UV and CD spectroscopic results suggested that they experienced a (supposedly irreversible) helix–helix conversion followed by a reversible helix–coil transition, the former of which proceeded under helix-sense inversion in the case of **P1**. Thus, the addition of TFA to the original blue-purple solution of poly(diacetylene) **P1** led to a color change to red-violet and, finally, yellow, associated with two distinct hypsochromic shifts of the highest wavelength UV absorptions by 70 and 60 nm associated with two isosbestic points at 536 and 469 nm, respectively (Figure 2, middle). It is important to note that, in contrast to many previous examples of the well-known poly(diacetylene) solvatochromism,<sup>32–37</sup> the red form was an actual intermediate with a clear spectroscopic signature and not a mixture of different species.<sup>49</sup> Accordingly, plots of the extinction ratios ( $\epsilon_{588}/\epsilon_{520}$  and  $\epsilon_{460}/\epsilon_{520}$  vs

vol % TFA) were consistent with two clearly consecutive and cooperative processes (Figure 4, top).

At the same time, the Raman spectra of **P1** (Figure 2, bottom) only showed minor changes in the absorption wavenumbers during the blue–red transition and remained almost unchanged during the red–yellow transition, implying that the solvatochromic transitions cannot be explained with altered conjugation lengths due to conformational changes *alone*.<sup>50</sup> The corresponding CD spectra (Figure 2, top) revealed that the addition of up to 0.6 vol % TFA led to a preliminary, almost complete disappearance of the bisignate CD signal at 588 nm, and this process was associated with a well-developed isosbestic point at the zero-crossing. At a cosolvent content of 0.6–1.2 vol % TFA, a new series of CD signals emerged at the position of the UV absorption bands of the red form of **P1**, which exhibited a *negative* Cotton effect and a zero-crossing at the position of the highest wavelength UV absorption combined with a *positive* CD activity near the position of the lower wavelength UV absorption maximum. In other words, the CD signatures of the blue and the red form of **P1** are inverted, from which a



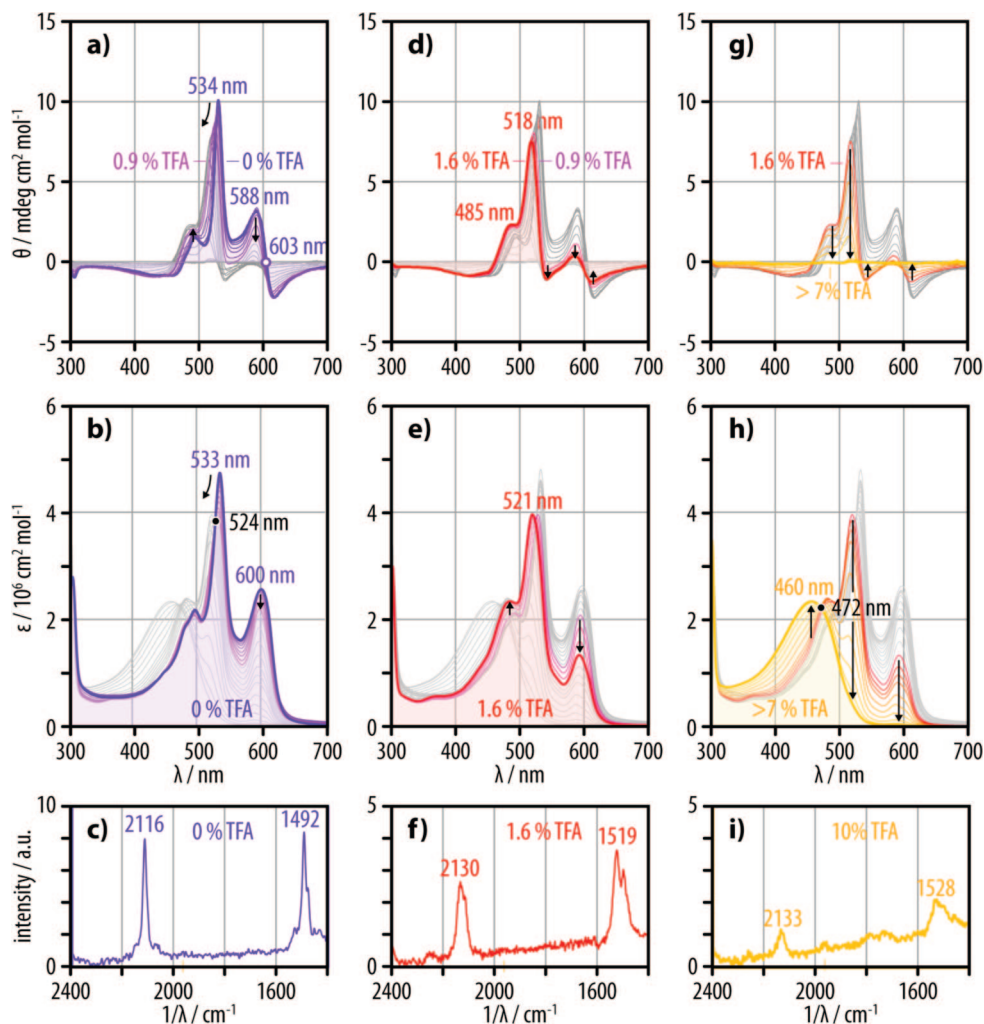


**Figure 3.** CD, UV, and Raman spectra of (a–c) the blue-purple solutions of **P2** after polymerization showed a mixture of the blue and the red form of **P2**, the former of which exhibited a *negative* Cotton effect; the addition of TFA led to (d–f) a solvatochromic transition to the red form, which also showed a *negative* Cotton effect; (g–i) addition of more TFA finally yielded the CD inactive yellow form.<sup>38</sup>

helix-sense inversion can be inferred. The CD activity of the red form reached a maximum at a volume fraction of around 1.2 vol % TFA, and further addition of TFA led to a successive decrease in CD activity until it completely disappeared in the regime of the yellow poly(diacetylene) solutions at volume ratios of about 2.5 vol % TFA and beyond.

Poly(diacetylene) **P2** showed essentially the same solvatochromic transitions, yet at higher cosolvent content. Furthermore, UV, CD, and Raman spectra (Figure 3), as well as plots of the extinction ratios (Figure 4b), were consistent with a more gradual interconversion and a coexistence of the three poly(diacetylene) species referred to as blue, red, and yellow form of **P2**. As mentioned above, the original blue-purple solution was already a mixture of two species, and the red-violet solution contained both the original blue form ( $\lambda_{\text{max}} = 600$  nm) and the new red form of **P2** ( $\lambda_{\text{max}} = 521$  nm). Only the yellow solutions at a TFA content of 7 vol % appeared to contain only one poly(diacetylene) species ( $\lambda_{\text{max}} = 460$  nm). As in the case of **P1**, the Raman spectra of **P2** (Figure 3, bottom) showed only marginal changes, in particular during the red–yellow transition. CD spectroscopy

revealed that both the blue and the red form of **P2** exhibited a *negative* Cotton effect for their respective highest wavelength UV absorptions. Hence, it seems that **P2** did not undergo a helix-sense inversion, and both the original blue form and the red form were, supposedly, left-handed helical *ribbons*. As the red species was already present in the original solution and the SFM images had shown two different types of left-handed helical *ribbons*, we tentatively assigned the blue form of **P2** to the major and its red form to the minor population of more tightly wound fibrils. As in the case of **P1**, the red–yellow transition was found to be associated with a complete loss of CD activity.

Finally, the transition from the red to the yellow form was found to be reversible upon the addition of triethylamine (TEA) as a base both in the case of **P1** and **P2** (Figure 5). Thus, the addition of only small amounts of TEA to the yellow solutions of **P1** and **P2** in DCE containing 2–6 vol % of TFA led to a color change back to deep red and an almost complete recovery of the UV and CD activity of the red forms of the two polymers (Figure 5). This process could even be repeated multiple times by addition of more TFA followed by small amounts of TEA. Interestingly, the “pure”

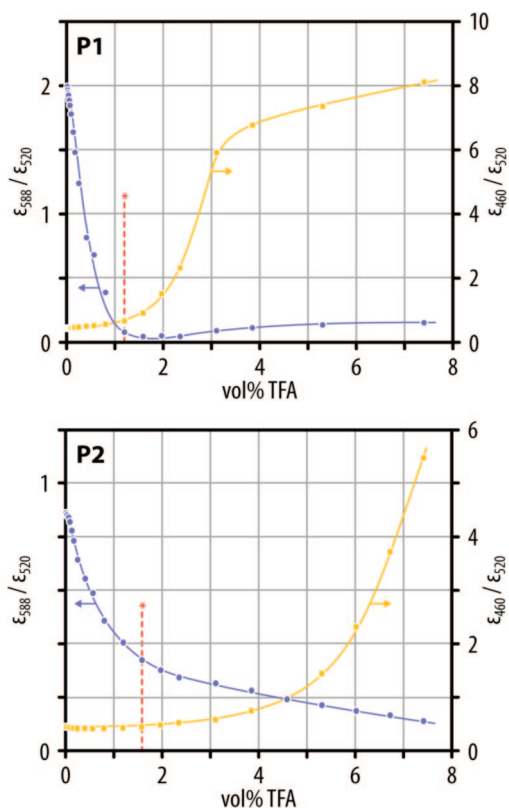


**Figure 4.** Plots of the extinction ratios at the UV absorption maxima of the blue, red, and yellow form of **P1** and **P2** as a function of TFA concentration. The blue curves are associated with the blue–red transition, the yellow curves with the red–yellow transitions, and the red asterisk denotes the cosolvent content at which the overall highest absorption for the red forms was observed.

red forms of **P1** and **P2** were obtained in this way, which exhibited a clear spectroscopic signature of essentially a single poly(diacetylene) species not contaminated with the blue (or the yellow) forms.

As noted above, the marginal changes in the Raman spectra suggested that the observed hypsochromic shifts in the UV absorptions can not only result from changes in the conjugation lengths due to conformational changes.<sup>48</sup> In particular, the drastic hypsochromic shifts in the course of the reversible red–yellow transition are not accompanied with any changes in the corresponding Raman spectra of **P1** and **P2** at all. Hence, one must conclude that the transitions were associated with a change in the aggregation state of the polymer chains as well. Furthermore, both the red and yellow forms of **P1** and **P2** were conspicuously similar in their UV, CD, and Raman spectroscopic properties (in particular, after treatment with TFA followed by TEA). Hence, it appears reasonable to assume that, after the initial blue–red transition, both poly(diacetylene)s attained very similar conformational states. In fact, one important feature of the original blue forms of **P1** and **P2** is that they are obtained in a *known* aggregation state with four and two helically wound poly(diacetylene) backbones, respectively. Consequently, **P1** appears to be converted from right-handed quadruple-helical *fibrils* to double-helical *ribbons* with left-handed helicity (as expected for stacked  $\beta$ -sheet ag-

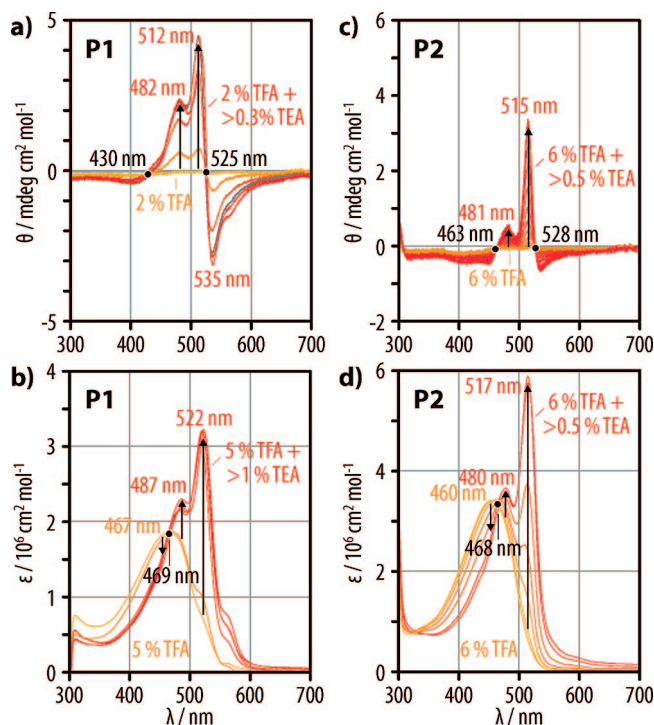


**Figure 5.** Upon addition of small amounts of TEA to the yellow solutions of **P1** or **P2** in DCE (containing TFA), the solutions turned red again, UV spectra proved the reformation of the red form of **P1** and **P2**, and the CD activity was recovered (isosbestic points marked in black).

gregates)<sup>40</sup> and, finally, to single random-coil poly(diacetylene)s (Figure 6). By contrast, one type of left-handed ribbons was converted into another one in the case of **P2**, which may be the reason for the observed more gradual interconversion and coexistence of different species. The helix–helix conversion under helix-sense inversion observed for **P1**, on the other hand, necessarily requires the right-handed double-helical bundles to be completely disentwined, either in one step or successively.

In conclusion, the hierarchically structured, oligopeptide-substituted poly(diacetylene)s described here were established as a new class of  $\pi$ -conjugated polymers with a defined, multiple-helical quaternary structure not only on surfaces but also in solution. The results represent one of the first correlations of the chiroptical properties of a  $\pi$ -conjugated polymer with its nanoscopic structure visualized by SFM. The polymers exhibited a rich dynamic folding behavior in solution that is currently unrivalled in the realm of synthetic foldamers. The solvatochromic transitions of this particular type of poly(diacetylene)s were shown to involve both distinct conformational transitions and (reversible) deaggregation. The irreversible first unfolding/deaggregation processes implied that the initial multiple-helical quaternary structures obtained via the chosen “*self-assemble then polymerize*” approach are unlikely to be accessible with the foldamer approach, regardless whether they are thermodynamic equilibrium structures or not. This highlights the role of supramolecular self-assembly as a pathway toward complex hierarchically structured synthetic polymer materials which exhibit optoelectronic activity.

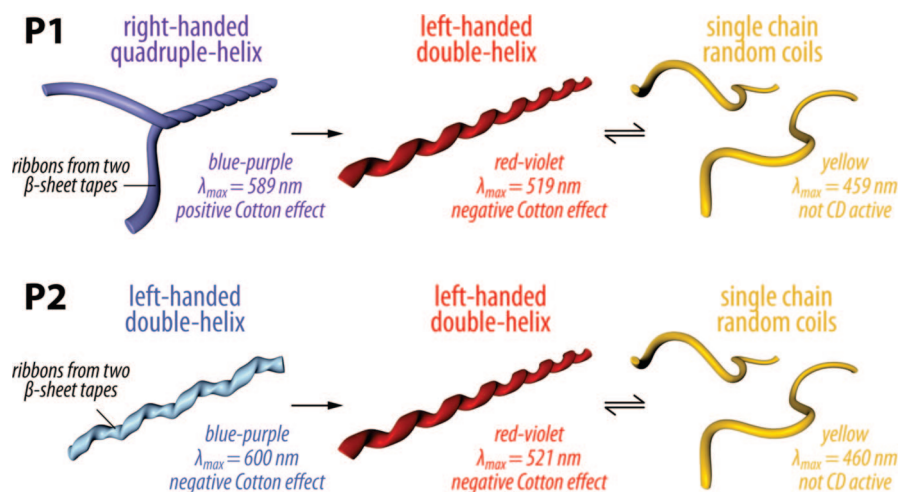


**Figure 6.** Schematic proposal for the changes in conformation and aggregation associated with the observed solvatochromic transitions of **P1** and **P2**.

**Acknowledgment.** We thank Prof. Peter B  uerle, Dr. Elena Mena-Osteritz, as well as Dr. G  nther G  tz (University of Ulm, Germany) for valuable discussions in relation to CD spectroscopy, and Prof. A. Dieter Schl  ter for his generous support. Funding from Fonds der Chemischen Industrie (Fonds-Stipendium, E. Jahnke), Schweizerischer Nationalfonds (SNF-Projekt 200021-113509), Deutscher Akademischer Austauschdienst (DAAD-Stipendium, J. Weiss), ETH Z  rich (Projekt TH-20 07-1), as well as Deutsche Forschungsgemeinschaft (Sfb 448 “Mesoscopically Organized Composites” and Sfb 658 “Elementary Processes in Molecular Switches at Surfaces”) is gratefully acknowledged.

**Supporting Information Available:** Enlarged SFM images, additional figures and comments, experimental procedures, as well as NMR and mass spectra of **1** and **2**. This material is available free of charge via the Internet at <http://pubs.acs.org>.

## References

- (1) Lakes, R. *Nature* **1993**, *361*, 511.
- (2) Hawker, C. J.; Wooley, K. L. *Science* **2005**, *309*, 1200.
- (3) Meijer, E. W.; Schenning, A. P. H. J. *Nature* **2002**, *419*, 353.
- (4) Gellman, S. H. *Acc. Chem. Res.* **1998**, *31*, 173.
- (5) Hill, D. J.; Mio, M. J.; Prince, R. B.; Hughes, T. S.; Moore, J. S. *Chem. Rev.* **2001**, *101*, 3893.
- (6) Cornelissen, J. J. L. M.; Donners, J. J. J. M.; de Gelder, R.; Graswinckel, W. S.; Metselaar, G. A.; Rowan, A. E.; Sommerdijk, N. A. J. M.; Nolte, R. J. M. *Science* **2001**, *293*, 676.
- (7) *Foldamers: Structure, Properties, and Applications*, 1st ed.; Hecht, S., Huc, I., Eds.; Wiley-VCH: Weinheim, Germany, 2007.
- (8) Nomura, R.; Tabei, J.; Masuda, T. *J. Am. Chem. Soc.* **2001**, *123*, 8430.
- (9) Zhao, H.; Sanda, F.; Masuda, T. *Macromolecules* **2004**, *37*, 8888.
- (10) Li, B. S.; Cheuk, K. K. L.; Ling, L.; Chen, J.; Xiao, X.; Bai, C.; Tang, B. Z. *Macromolecules* **2003**, *36*, 77.
- (11) Cheuk, K. K. L.; Lam, J. W. Y.; Lai, L. M.; Dong, Y.; Tang, B. Z. *Macromolecules* **2003**, *36*, 9752.
- (12) Percec, V.; Aqad, E.; Peterca, M.; Rudick, J. G.; Lemon, L.; Ronda, J. C.; De, B. B.; Heiney, P. A.; Meijer, E. W. *J. Am. Chem. Soc.* **2006**, *128*, 16365.
- (13) Sakai, R.; Otsuka, I.; Satoh, T.; Kakuchi, R.; Kaga, H.; Kakuchi, T. *Macromolecules* **2006**, *39*, 4032.
- (14) Jahnke, E.; Lieberwirth, I.; Severin, N.; Rabe, J. P.; Frauenrath, H. *Angew. Chem., Int. Ed.* **2006**, *45*, 5383.
- (15) Brunsveld, L.; Folmer, B. J. B.; Meijer, E. W.; Sijbesma, R. P. *Chem. Rev.* **2001**, *101*, 4071.
- (16) Georger, J. H.; Singh, A.; Price, R. R.; Schnur, J. M.; Yager, P.; Schoen, P. E. *J. Am. Chem. Soc.* **1987**, *109*, 6169.
- (17) Spector, M. S.; Selinger, J. V.; Singh, A.; Rodriguez, J. M.; Price, R. R.; Schnur, J. M. *Langmuir* **1998**, *14*, 3493.
- (18) Singh, A.; Wong, E. M.; Schnur, J. M. *Langmuir* **2003**, *19*, 1888.
- (19) Svenson, S.; Messersmith, P. B. *Langmuir* **1999**, *15*, 4464.
- (20) Cheng, Q.; Yamamoto, M.; Stevens, R. C. *Langmuir* **2000**, *16*, 5333.
- (21) Frankel, D. A.; O'Brien, D. F. *J. Am. Chem. Soc.* **1991**, *113*, 7436.
- (22) Fuhrhop, J. H.; Blumtritt, P.; Lehmann, C.; Luger, P. *J. Am. Chem. Soc.* **1991**, *113*, 7437.
- (23) Masuda, M.; Hanada, T.; Yase, K.; Shimizu, T. *Macromolecules* **1998**, *31*, 9403.
- (24) Tamaoki, N.; Shimada, S.; Okada, Y.; Belaisaoui, A.; Kruk, G.; Yase, K.; Matsuda, H. *Langmuir* **2000**, *16*, 7545.
- (25) Nagasawa, J.; Kudo, M.; Hayashi, S.; Tamaoki, N. *Langmuir* **2004**, *20*, 7907.
- (26) Aoki, K.; Kudo, M.; Tamaoki, N. *Org. Lett.* **2004**, *6*, 4009.
- (27) Yuan, Z.; Lee, C.-W.; Lee, S.-H. *Angew. Chem., Int. Ed.* **2004**, *43*, 4197.
- (28) Dautel, O. J.; Robitzer, M.; Lere-Porte, J. P.; Serein-Spirau, F.; Moreau, J. J. E. *J. Am. Chem. Soc.* **2006**, *128*, 16213.
- (29) Jahnke, E.; Kreutzkamp, P.; Severin, N.; Rabe, J. P.; Frauenrath, H. *Adv. Mater.* **2008**, *20*, 409.
- (30) Frauenrath, H.; Jahnke, E. *Chem. Eur. J.* **2008**, *14*, 2942.
- (31) Weiss, J.; Jahnke, E.; Frauenrath, H. *Macromol. Rapid Commun.* **2008**, *29*, 330.
- (32) Patel, G. N.; Chance, R. R.; Witt, J. D. *J. Chem. Phys.* **1979**, *70*, 4387.
- (33) Chance, R. R. *Macromolecules* **1980**, *13*, 396.
- (34) Berlinsky, A. J.; Wudl, F.; Lim, K. C.; Fincher, C. R.; Heeger, A. J. *J. Polym. Sci., Polym. Phys. Ed.* **1984**, *22*, 847.
- (35) Wenz, G.; M  ller, M. A.; Schmidt, M.; Wegner, G. *Macromolecules* **1984**, *17*, 837.
- (36) Drake, A. F.; Udvarhelyi, P.; Ando, D. J.; Bloor, D.; Obhi, J. S.; Mann, S. *Polymer* **1989**, *30*, 1063.
- (37) Deb, P.; Yuan, Z.; Ramsey, L.; Hanks, T. W. *Macromolecules* **2007**, *40*, 3533.
- (38) See Supporting Information.
- (39) Severin, N.; Barner, J.; Kalachev, A.; Rabe, J. P. *Nano Lett.* **2004**, *4*, 577.
- (40) Aggeli, A.; Nyrkova, I. A.; Bell, M.; Harding, R.; Carrick, L.; McLeish, T. C. B.; Semenov, A. N.; Boden, N. *Proc. Natl. Acad. Sci. U.S.A.* **2001**, *98*, 11857.
- (41) Consistent with our own self-assembly model (ref 29) and in analogy to the model proposed by Boden et al. (ref 40), the terms *tapes*, *ribbons*, and *fibrils* are explicitly used to describe single  $\beta$ -sheets, stacked dimers of  $\beta$ -sheets, as well as higher aggregates via stacking of  $\beta$ -sheets, respectively.
- (42) Wegner, G. Z. *Naturforsch., B: Chem. Sci.* **1969**, *24*, 824.
- (43) Sakurai, S.-I.; Okoshi, K.; Kumaki, J.; Yashima, E. *Angew. Chem., Int. Ed.* **2006**, *45*, 1245.
- (44) Pons, M.; Johnston, D. S.; Chapman, D. *J. Polym. Sci., Polym. Chem. Ed.* **1982**, *20*, 513.
- (45) Johnston, D. S.; McLean, L. R.; Whittam, M. A.; Clark, A. D.; Chapman, D. *Biochemistry* **1983**, *22*, 3194.

- (46) Song, J.; Cheng, Q.; Kopta, S.; Stevens, R. C. *J. Am. Chem. Soc.* **2001**, *123*, 3205.
- (47) Huang, X.; Liu, M. *Chem. Commun.* **2003**, 66–67.
- (48) A few reports concerning the CD activity of poly(diacetylene)s have been published previously (refs 36, 37, 44–47). With the exception of the investigations by Ando et al. and Hanks et al. (refs 36 and 37), however, only poorly defined CD signatures were observed that were typically not interpretable and probably resulted from a circular intensity differential scattering (cids) contribution of large, ill-defined superstructures. This conclusion is, for example, illustrated by the results reported by Liu et al. (ref 47), who observed CD activity in LB films of achiral poly(diacetylene)s; the CD activity was irreproducible and depended, e.g., on the subphase; TEM images showed supposedly helical superstructures with a pitch on the order of the wavelength of the absorbed light. For more information on cids, see Bustamante, C. Tinoco, I., Jr.; Maestre, M. F. *Proc. Natl. Acad. Sci. U.S.A.* **1983**, *80*, 3568.
- (49) The color changes may look similar to previously published examples (refs 32–35) at first sight, but there are important differences. Solutions of **P1** or **P2** in chlorinated solvents maintained their blue-purple color, and only the addition of strong hydrogen bond breaking agents induced the color changes. The transition from the blue to the yellow form clearly proceeded in two consecutive steps, with the red form as an actual intermediate. A similar supposedly two-step transition was recently described by Dautel, Moreau et al. (ref 28), but the reported UV spectra showed mixtures of different species and were, hence, difficult to interpret.
- (50) Giesa et al. have conclusively shown that this explanation falls short anyway; UV absorption maxima above about 550 nm probably result from interactions of poly(diacetylene) chromophores in the crystalline or aggregated state; see Giesa, R. R. Schulz, C. *Polym. Int.* **1994**, *33*, 43.

NL080478H